EIT Reconstruction of A Two-Dimensional Flow Field Using Regularized Newton-Raphson Method

Jae-Woo Park*, Kyung-Youn Kim** and Yoon-Joon Lee*

정규화 Newton-Raphson 법을 사용한 2차원 유동장의 EIT 영상복원

박 재 우* · 김 경 연** · 이 윤 준*

ABSTRACT

The regularized Newton-Raphson method(RNRM) has been used to reconstruct by electrical impedance tomography (EIT) a two-dimensional flow field containing some artificial objects. Three different cases of object size, number and position were investigated. Instead of using measured voltage data at boundary electrodes, computed data were used. It is found that the reconstruction method employed is working well for the three cases. Though some blurring is found along the contour of the objects, the overall shape of the objects can be well reconstructed. The position of the objects was also accurately predicted. Also investigated is the effect of the regularization parameter. Our study shows the use of smaller regularization parameter results in better reconstruction.

Key Words : regularized Newton-Raphson method, EIT, regularizatiopn parameter

I. INTRODUCTION

The EIT (Electrical Impedance Tomography) technology has become a potential tool for reconstructing the phase distribution of a two-phase flow field. The major advantage of an EIT system is that its temporal resolution is higher than other tomographic measuring techniques such as X-ray CT (computer tomography) or ultrasonic tomography. Time resolutions more than 50 frames per second can be achieved. In an EIT system, a number of electrodes are mounted on the periphery of the flow field which contain an electrically conducting medium such as ordinary water. A prescribed electric current is injected into one electrode, known as the source electrode, and withdrawn at another electrode or sink electrode which is usually grounded. The resulting electric voltages are then measured at all of the electrodes with respect to the ground. The measured voltages are dependent on the conductivity

* 제주대학교 에너지공학과, 첨단기술연구소
  Department of Nuclear and Energy Engineering, Research Institute of Advanced Technology, Cheju Nat'l Univ.
** 제주대학교 전자공학과, 첨단기술연구소
  Department of Electronic Engineering, Research Institute of Advanced Technology, Cheju Nat'l Univ.

(or resistivity) distribution of the flow field. For a bubbly two-phase flow mixed with water and air, for instance, the conductivity difference between water and air is very large, so that it is possible to infer the phase distribution from the measured voltages on the boundary electrodes.

The reconstruction problem basically includes forward and inverse solution steps. In the forward solution step, the electric potential distribution inside the flow domain and on the periphery is computed based on an assumed conductivity distribution. Though nonlinear, the forward problem is well-conditioned, and there exists a unique solution. Efficient methods, for instance the FEM(finite element method), are available to convert the forward problem into a system of linear algebraic equations. One can either write his own FEM program or use a commercial tool such as MATLAB to solve the forward problem.

In the inverse solution step, the interior conductivity distribution is reconstructed from the measured voltages on the boundary. The inverse problem is ill-conditioned in nature and hence there does not generally exists a unique solution corresponding to a boundary voltage distribution. Approaches for solving the inverse problem can be categorized as direct and iterative methods. Direct analytical solution methods are subject to simplifying assumptions and their usage in the case of two phase flow fields is of very little practical interest. In iterative approaches, a candidate conductivity distribution is first assumed. A set of boundary voltage values are then calculated from the candidate distribution by solving the forward problem. The calculated voltages are compared to voltages measured on the boundary during current injection, and the reconstruction error is represented in the form of their squared difference. The candidate conductivity distribution is then modified based on the error. The forward problem is again

solved based on the modified conductivity distribution, and new reconstruction error is evaluated. This process is continued until some error criterion is satisfied.

Various reconstruction methods have been developed and applied to reconstructing the phase distribution of multiphase flows. Methods of more frequent application include the back projection method[1], the Newton's one-step error reconstruction (NOSER) method[2], Newton-Raphson method (RNM)[3]. A comprehensive description of these methods can be found in references[4]. These methods are basically the same in the sense they generally follow the procedures described in the last paragraph. They differ in the way the current conductivity distribution is updated to obtain a new distribution.

Yorkey et al.[5] developed a modified version of Newton-Raphson method, also known as the YWT method, and much reconstruction work has been done with this method. It is reported that the modified Newton-Raphson method has produced more accurate results than any other method listed above when there exists no noise. However, its performance worsens when measurement noise is present. It produces noisy images when the number of elements are large for good spatial resolution.[4] In order to compensate these drawbacks, Hua et al.[6] introduced including a regularization term in the reconstruction error. Several methods of the regularization have been suggested.

We have implemented the Newton-Raphson algorithm regularized by the subspace regularization method suggested by Vauhkonen[7]. In this paper, we present reconstructed images of a circular flow field which is assumed to contain artificial object of different conductivity. Also presented are the effect of the regularization parameter on the reconstructed images and the transient behavior of the relative root mean square error of the reconstruction.

II. FORWARD PROBLEM

In a conducting medium where no charge sources or sinks are present, the governing equation for the electric field can be derived from Maxwell's equation as

$$\nabla \cdot \sigma \nabla \phi = 0 \qquad (1)$$

where σ is the conductivity distribution of the medium and ϕ is the electric potential. For an EIT system with finite number of discrete electrodes mounted on the periphery of the flow field, the boundary conditions are given by

$$\boldsymbol{n} \cdot \sigma \nabla \phi = \begin{cases} -q & \text{on } \Omega_E \\ 0 & \text{on } \Omega_H \end{cases} \qquad (2)$$

where $\boldsymbol{n}$ is the outward unit normal vector on the bounding surface, and q is the current density at the boundary. Ω_E and Ω_H denote the surface of the excitation electrodes and the rest of the boundary surface, respectively.

For FEM modeling of eq. (1), the flow domain is divided into a finite number of elements. Since our problem is two dimensional, we use triangular elements. It is assumed that the conductivity distribution is constant in each element, and the potential distribution in an element can be represented by a simple interpolation formula:

$$\phi(x, y) = \sum_i \phi_i f_i(x, y) \qquad (3)$$

where ϕ_i are the potentials at nodes(vertices) of the triangular element. $f_i(x, y)$ is a dimensionless interpolation function which has the value 1 at the i-th node and 0 at other two nodes. Given the boundary conditions and with the treatment of eq. (3), Eq. (1) can be converted into a system of algebraic equations of the form[7]:

$$A b = f \qquad (4)$$

where A is the admittance matrix of dimension $(N+L-1) \times (N+L-1)$ with N and L being the number of internal nodes and the number of electrodes, respectively. b and f are the vectors of the electrical potential(ϕ) and current density(j), respectively.

$$b = (\phi_1, \phi_2, \ldots \phi_{N+L-1})^T \qquad (5)$$

$$f = (i_1, i_2, \ldots i_{N+L-1})^T \qquad (6)$$

Elements of the vector f become zero except at source and sink electrodes.

Thus, given the conductivity distribution and boundary conditions, eq. (1) can be uniquely solved, and the solution provides the voltage values at all nodes including the boundary electrodes. We use the MATLAB to solve the forward problem.

III. INVERSE PROBLEM

The goal of the inverse solution step is to seek a resistivity (or conductivity) distribution which minimizes the difference between measured and computed voltages at the boundary electrodes. In order to do this, the resistivity distribution used in the forward solution step is continuously updated based on the voltage difference. The Newton-Raphson method(RNM) takes the objective function as

$$\Phi(\rho) = \frac{1}{2} [V(\rho) - U]^T [V(\rho) - U] \qquad (7)$$

where $V(\rho)$ and U are vectors of the computed and measured voltages, respectively, at the boundary electrodes. ρ is the resistivity distribution of the flow medium defined by $\rho = \sigma^{-1}$. The vectors $V(\rho)$ and U are defined as

$$V = [v_1^1, v_2^1, \ldots, v_1^2, v_2^2, \ldots, v_j^i, \ldots]^T$$
$$j = 1, 2, \ldots, Q, \quad i = 1, 2, \ldots, P \qquad (8)$$

$$U = [u_1^1, u_2^1, \ldots, u_1^2, u_2^2, \ldots, u_j^i, \ldots]^T$$
$$j = 1, 2, \ldots, Q, \quad i = 1, 2, \ldots, P \tag{9}$$

where

v_j^i = computed voltage at the j-th electrode for the i-th injected current

u_j^i = measured voltage at the j-th electrode for the i-th injected current

Q = the number of electrodes

P = the number of injected current patterns

Minimization of the objective function requires:

$$\Phi'(\rho) = [V'(\rho)]^T [V(\rho) - U] = 0 \tag{10}$$

where the first derivative term $V'(\sigma)$ is called the Jacobian matrix and defined as

$$J = V'(\rho) = \frac{\partial V_i}{\partial \rho_j},$$
$$i = 1, 2, \ldots, Q \times P, \quad j = 1, 2, \ldots, M \tag{11}$$

where ρ_j is the conductivity of the j-th element and M is the number of mesh elements used.

The Taylor's series expansion of $\Phi'(\rho)$ at $\rho^{k+1} = \rho^k + \Delta\rho^k$ is approximated by

$$\Phi'(\rho^{k+1}) \approx \Phi'(\rho^k) + \Phi''(\rho^k)\Delta\rho^k = 0 \tag{12}$$

The second derivative term Φ'' is called the Hessian matrix and can be approximated as

$$H_{M \times M} = \Phi''(\rho^k) \approx [V'(\rho^k)]^T V'(\rho^k) = J^T J \tag{13}$$

where we have neglected the second derivative of $V(\rho^k)$. Rearranging eq. (12) gives

$$\Delta\rho^k = \rho^{k+1} - \rho^k = -H^{-1}J^T[V(\rho^k) - U] \tag{14}$$

During minimizing of the objective function by the RNM, high ill-conditioning occurs due to a very high condition number of the Hessian matrix, which is defined as the ratio of the maximum eigenvalue

to the minimum. Usual approach to overcome this problem is to include a regularization term in the objective function. We use the regularized Newton-Raphson method(RNRM) where the objective function is given by

$$\Phi(\rho) = \frac{1}{2}[V(\rho) - U]^T[V(\rho) - U] + \frac{1}{2}\alpha(L\rho)^T(L\rho) \tag{15}$$

where α and L are the regularization parameter and the regularization matrix, respectively. By following the same procedure as used above, we can get

$$\Delta\rho^k = \rho^{k+1} - \rho^k$$
$$= -(H + \alpha L^T L)^{-1}\{J^T[V(\rho^k) - U] + \alpha L^T L\rho^k\} \tag{16}$$

Various methods of specifying the regularization matrix are available. For instance, the algorithm[4] developed by Rensselaer Polytechnic Institute uses $L^T L = diag(J^T J)$. We use the subspace regularization method the detail of which is given in reference[7].

The majority of the computational effort using the RNM is involved with the calculation of the Jacobian matrix, and subsequently the Hessian. From eqs (4) and (11), the derivative of the potential distribution with respect to the resistivity of the n-th element can be obtained by

$$\frac{\partial b}{\partial \rho_n} = \frac{\partial(A^{-1}f)}{\partial \rho_n} \tag{17}$$

where ρ_n is the resistivity of the n-th element. The right hand side of eq. (17) can be expanded as

$$\frac{\partial(A^{-1}f)}{\partial \rho_n} = -A^{-1}\frac{\partial A}{\partial \rho_n}A^{-1}f = -A^{-1}\frac{\partial A}{\partial \rho_n}b \tag{18}$$

The derivative of the admittance matrix is can be calculated as

$$\frac{\partial A(m, i)}{\partial \rho_n} = -\frac{1}{\rho_n^2} \int_{\Delta_n} \nabla \phi_m \cdot \nabla \phi_i \qquad (19)$$

where

$A(m, i)$ = element of A at m-th row and i-th column

$\nabla \phi_m$ = the gradient of the m-th node basis function

Δ_n = integration over the n-th element

Since eq. (17) forms the derivatives of all the voltages, the Jacobian is constructed with the part which belongs to the electrode nodes. After the Jacobian matrix has been obtained, the Hessian matrix can be constructed by eq. (13). Now we can solve eq. (16) and update the resistivity distribution using the relation

$$\rho^{k+1} = \rho^k + \Delta\rho^k \qquad (20)$$

where k is the iteration count. In order to check the convergence of a reconstruction during iteration, the root mean square error(RMSE) is usually evaluated by

$$RMSE = \sqrt{\frac{[U_k - V_k(\rho_k)]^T \cdot [U_k - V_k(\rho_k)]}{U_k^T \cdot U_k}} \qquad (21)$$

IV. NUMERICAL EXPERIMENTS

In order to examine the performance of the RNRM, we have considered a two-dimensional circular flow field with a diameter of 30 cm and 16 electrodes equidistantly spaced on the periphery. It is assumed that one reference electrode(sink electrode) is fixed to ground while the rest of the electrodes serve as the current source. For each current injection, the true voltages are computed at all electrodes by solving eq. (1). The MATLAB is used for FEM mesh generation and solution of eq.

(4). For numerical experiments these computed voltage data are used as measured data.
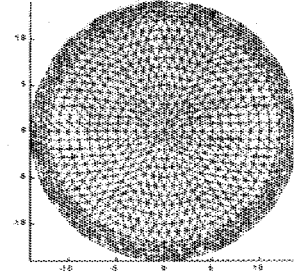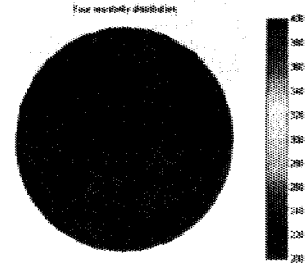

Fig. 1. The FEM mesh structure.
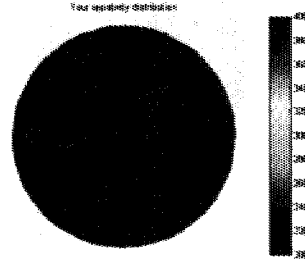

Fig. 2(a). True view of case 1.
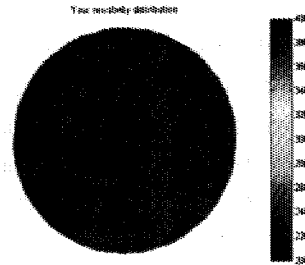

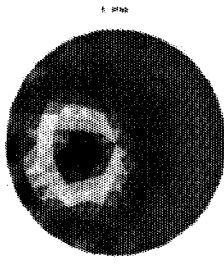Fig. 2(b). True view of case 2.

Fig. 2(c). True view of case 3.

Fig. 3(a). Reconstructed image of case 1
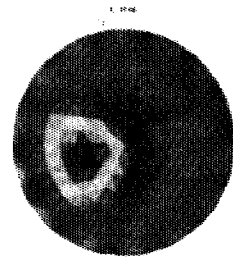(α = 0.0005).

Fig. 4(a). Reconstructed image of case 1
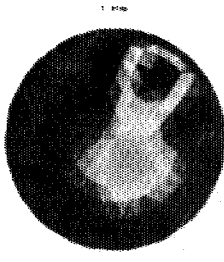(α = 0.000005).

Fig. 3(b). Reconstructed image of case 2
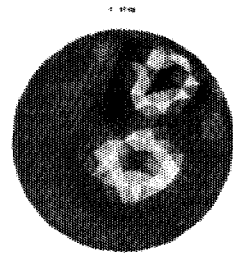(α = 0.0005).

Fig. 4(b). Reconstructed image of case 2
(α = 0.000005).

Fig. 3(c). Reconstructed image of case 3
(α = 0.0005).

Fig. 4(c). Reconstructed image of case 3
(α = 0.000005).

We have considered 3 cases of fictitious flow regimes which contain a bulk medium of resistivity 400 Ωcm and artificial objects of resistivity 200 Ωcm. Fig. 1 shows the mesh structure used, wherein 1968 triangular elements and 1049 nodes are constructed. In the first case, Fig. 2 (a), we assume an artificial object of relatively large size located between the center and the periphery. The second case, Fig. 2 (b), contains two small objects: one located around

the center and the other near the periphery. The third case, Fig. 2 (c), also contains two small objects: both of them lying near the periphery.

In order to examine the effect of the regularization parameter(α) on the reconstruction we tested two values: $\alpha = 0.0005$ and $\alpha = 0.000005$. The initial candidate resistivity distribution were $\rho = 400$ Ωcm in all elements. Figs. 3 (a), (b), (c) show reconstructed images of cases 1, 2 and 3, respectively
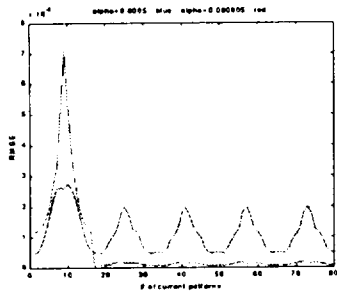
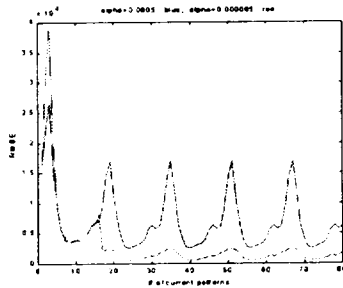Fig. 5(a). Root mean square error of the case 1 reconstruction.

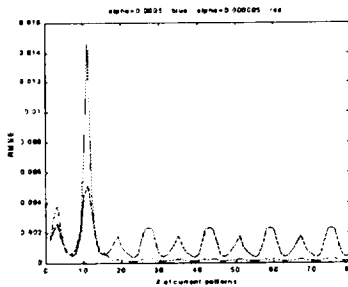Fig. 5(b). Root mean square error of the case 2 reconstruction.

Fig. 5(c). Root mean square error of the case 3 reconstruction.

when $\alpha = 0.0005$. The images shown in Figs. 4 were obtained with $\alpha = 0.000005$. It is found that the reconstruction method we have used works fine for the 3 cases. Although some blurring is found along the boundary of the objects, one can generally identify the contour of the objects. The positions of

the objects and reconstructed images well match.

As for the effect of the regularization parameter, it is evident that the use of the smaller α results in better reconstruction. The effect is better shown in Figs. 5 (a), (b), (c), where the RMSE's are compared for both α values. With $\alpha = 0.000005$ the RMSE's for the 3 cases sharply drop and become stable with 20 current patterns. With $\alpha = 0.0005$, however, the RMSE's oscillate even after a large number of current patterns are used.

V. CONCLUSION

The regularized Newton-Raphson method has been used to reconstruct a two-dimensional flow field with some artificial objects. Three different cases of object number, size and position were investigated by numerical experiments. Instead of using actually measured voltage data at electrodes, computed voltage data were used. The data were obtained by solving the governing equation with MATLAB. It is found that the reconstruction method employed works fine for the 3 cases. Although some blurring is found along the boundary of the objects, the shape of the objects can be well identified. The positional accuracy is also very good. As for the effect of the regularization parameter, the use of the smaller regularization parameter results in better reconstruction. It is found proper choice of the regularization parameter is important to reduce computational efforts as well as experimental work.

Further research is needed to improve the spatial resolution of the reconstructed image, especially when more than two objects are close to each other. Also needed is further investigation of the effect of the regularization parameter and regularization matrix.

7

요 약

이물질을 포함하는 2차원 유동장에서 정규화 Nwton-Raphson 기법을 이용하여 전기임피던스 단층 촬영에 의한 영상복원을 시도하였다. 서로 다른 크기, 위치, 개수를 갖는 시스템에 대해, 전산모사 데이터를 이용하여 영상복원을 한 결과, 만족할 만한 결과를 얻었다. 대상체에 대한 영상이 다소 회미하였으나 전 체적인 대상체의 크기와 위치는 충분히 판별할 수 있 을 정도였다. 또한, 정규화 매개변수가 복원 결과에 미치는 영향을 살펴보았으며, 본 연구의 범위에서 그 크기가 작을수록 복원된 영상의 질이 개선되었다.

REFERENCES

1) D. C. Barber, B. H. Brown, and I. L. Freeston. 1983. Imaging Spatial Distribution of Resistivity using Applied Tomography. Elec. Lett., Vol. 19, pp. 446-462.

2) M. Cheney, D. Isaacson, J. C. Newell, S. Simske, and J. Goble, 1990. NOSER: An Algorithm for Solving Inverse Conductivity Problem. Int. J. Imag. Sys. and Tech., Vol. 2, pp. 66-75.

3) T. J. Yorkey. 1986. Comparing Reconstruction Methods for Electrical Impedance Tomography. Ph.D. Thesis. Department of Electrical Computer Engineering. University of Wisconsin. Madison. WI.

4) L. Ovacik and O. C. Jones, 1998. Development of an Electrical Impedance Computed Tomographic Two-Phase Flows Analyzer. Final Report, Department of Nuclear Engineering and Engineering Physics. Rensselaer Polytechnic Institute. Troy, New York.

5) T. J. Yorkey, J. G. Webster, and W. J. Tompkins. 1987. Comparing Reconstruction Methods for Electrical Impedance Tomography. IEEE Transanction on Biomedical Engineering. Vol. 11., pp. 843-852.

6) P. Hua, J. G. Webster, and W. J. Tompkins, 1988. A Regularized Electrical Impedance Tomography Reconstruction Algorithm. Clin. Phys. Physiol. Meas., Vol. 8. Suppl. A. pp. 137-141.

7) M. Vauhkonen, 1997. Electrical Impedance Tomography and Prior Information. ISSN 1235-0486. Kupio University Publishings Co.